Explicit and Implicit Simulations for Die-Less-Hydroforming-Structures including Welding, Forming and Load Capacity using LS-DYNA® and DynaWeld®

Andreas Metzger, Thomas Ummenhofer
Karlsruhe Institute of Technology, KIT Steel & Lightweight Structures,
Research Center for Steel, Timber & Masonry
Otto-Ammann-Platz 1, 76131 Karlsruhe, Germany

Abstract

Within the scope of Die-Less-Hydroforming, two or more flat metal blanks that have the same cutting-geometry are stacked congruently one above the other, and are then seal-welded on their common edges. Afterwards, the resulting seal-welded double- or multi-layered blank is inflated by a medium (e.g. water) whereby it transforms to a spatial structure under continuous internal pressure increase. Since no external forming tool is used, and because of the thin blank sheets (ranging from 0.5 up to 4mm), Die-Less-Hydroforming is very sensitive to buckling phenomena. Although this unconventional forming technology (also known under some synonyms, e.g. inflating metals) was first mentioned in the academic discourse in the 1920s [1], it is currently very up-to-date among many users, and versatile applications in different fields are developing.

In this contribution, we want to continue reporting on our previously presented research work on the simulation of welding and forming [2] by suggesting the manufacturing of some customized tubular load bearing structures by Die-Less-Hydroforming, which makes it necessary to prepare the resulting FEM-object for the transfer to the subsequent determination of the load capacity.

Consequently, a process chain simulation for Die-Less-Hydroforming Structures is presented, including the thermo-structural-mechanical welding simulation (LS-DYNA implicit and DynaWeld® for preprocessing), the time- and mass-scaled forming simulation (LS-DYNA explicit) and the preparation steps for transferring them to a load capacity simulation (LS-DYNA implicit), by always using the well-known dynain-file for transferring the required information between the different steps.

1. Introduction, motivation and some technical background

In this paper we focus on one of the simplest "Die-Less-Hydroforming"-structure consisting of a double-layered strip-shaped blank at the initial state. Strip-shaped means, that the double-layered blank is of rectangular shape with a length L that is many times longer than its width B. By inflating this double-layered strip-shaped blank it transforms, combined with stiffness increase, to a tubular structure with almost a circular cross section in a subsequent state which could be used as a thin-walled bar structure (e.g. for axial compression load). The main idea by doing this is to offer an opportunity for the manufacturing of customized tubular structures, especially for those that cannot deliver from storage by default due to reasons of extraordinary dimension concerning wall thickness, diameter or special material grade (especially stainless steel). Even the manufacturing of a custom-made tubular structure with a changeable cross section is possible.

The efficient possibility of a one-of-a-kind fabrication or a small-batch-production will be one of the greatest benefits using Die-Less-Hydroforming, especially with building applications, which often require only one or a small number of identical, but specific construction components. This was already recognized and supposed by B. Rawling in the 1960s [3]. The combination of the simple materials (some congruent blanks of arbitrary geometry) and the required equipment (a standard manual welding machine and a pressure pump in the range from 1 to 300 bar, which is very low in comparison to the working pressure required for conventional hydroforming) makes Die-Less-Hydroforming to a fast growing forming technology with a very innovative development potential. For the fabrication of fluid conducting pipes from double-layered strip-shaped blanks by using Die-Less-Hydroforming extensive research was already conducted in the 1990s [4].

Looking in detail to the manufacturing of the double-layered strip-shaped blank, some specific characteristics can be found that require the development of a process chain simulation. A short summary of the discussion of these procedures as well as some technical specifications taken from [5] is given in the following.

The two superposed blanks are welded at their common edges with a seal-weld. It is beyond any question that the welding parameters and especially the quality of these seal-welds have a big influence on the following forming process. On the one hand, the weld quality generally influences the possible forming grade, which means that high-quality welding will allow a wide-running forming process up to bursting that can even occur in the base material of the blank. However, lower weld-quality will end up in failures at an early state of inflation, in particular often by fine cracks in the weld seam (with continuous splashing water from within) or by an abrupt failure in terms of weld seam fracture over a longer part of the weld seam.

On the other hand, the welding process with transient heat flux in particular with thin metal sheets, results in welding distortions and/or welding residual stresses that generally occur after cooling down. Especially for our specific double-layered strip-shaped blank with long weld seams in longitudinal direction, an axial shrinking force develops during cooling down. These shrinking forces on both sides lead to an extensive compression stress zone in the blank area in-between the longitudinal seal-welds. The value of these shrinking forces mainly depends on the energy input per unit length during welding and on the size of the weld. If the shrinking forces and the resulting compression stress reach a critical value, stability phenomena which manifests in form of an extensive buckling pattern will occur.

This is precisely what can be observed in Fig. 1(a) and Fig. 2(a) for real samples, which feature visible welding distortions in the form of a characteristic buckling pattern as well as an invisible residual stress state.

Certainly, for the manufacturing of technically suitable tubular structures, such strong distortions like a buckling pattern of the complete double-layered Die-Less-Hydroforming blank, as shown in Fig. 1(a), have to be avoided. Such strong welding distortions influence the subsequent forming process, the formation of wrinkles is in particular abetted, which can be observed in the image sequence in Fig. 1(b)-(d). However, for academic reasons it will definitely be interesting to look at the influence of such a buckling pattern as well as the welding residual stresses to the subsequent forming step. We can profit from the simulation results at least for planning the manufacturing process (e.g. for determining useful welding parameters).

(a) **(b)** **(c)** **(d)**

Fig. 1: Strip-shaped Die-Less-Hydroforming sample with welding distortions in terms of a buckle pattern after welding at initial state (a) and here from the development of some wrinkles during the subsequent inflation process (b), (c) & (d) (Image source: Bachelor thesis at Karlsruhe Institute of Technology, KIT Steel & Lightweight Structures, Research Center for Steel, Timber & Masonry)

When inflating an ideal (i.e. suitable welded with few welding residual stresses and distortions) double-layered blank in reality and the corresponding perfect blank with nominal dimensions (and without any residual stresses and distortions) in the simulation, we can observe another specific buckling phenomena occurring independently in a strip-shaped zone near the weld and the heat affected zone (HAZ) under compressive stresses. These buckling phenomena are very characteristic for strip-shaped Die-Less-Hydroforming samples, c.f. Fig. 2 (b), and are mainly controlled by the relation of thickness to the dimensions width and length.
These two buckling phenomena described above are generally independent, but the welding distortions (in the worst case consisting of a heavy buckling pattern as shown in Fig. 1(a)) and the welding residual stresses influence the subsequent forming process anyway. Furthermore, by simulating the manufacturing sequence (including welding and forming) a realistic mesh geometry including deformations, thickness, residual stresses and strains is achieved. This will be especially beneficial when using the resulting Die-Less-Hydroforming object as a tubular structure. The determination of the load capacity in following depends strongly on these features.

(a) initial state with a smooth buckling pattern due to welding

(b) characteristic buckling due to the relation of thickness to the dimensions width and length

Fig. 2: Inflation sequence of a strip-shaped Die-Less-Hydroforming double-layered blank (Image source: Screenshots from https://youtu.be/eA46WFX7jWA FIREWORK SAFETY SUIT-Stand INSIDE a fireworks display [6], work of Colin Furze [7], for further details see also http://www.colinfurze.com/hydroforming.html)

2. Modeling details

The general modeling approach in Fig. 3 was already presented by the authors inter alia in [2], [8] and can be used for any arbitrary double-layered blank in the thermo-structural-mechanical welding simulation and in the Die-Less-Hydroforming simulation.
The model for the double-layered "Die-Less-Hydroforming" blank is built up by meshing the blanks with 4-Node Belytschko-Tsay shell elements using LS-PrePost®. The weld seam is modeled by fold all edge element rows of both blanks and afterwards merging the duplicated nodes. By doing this, the weld seam is modeled technically suitable as well as computationally feasible and a closed control volume is achieved, that is necessary for the subsequent forming simulation at initial state.
For setting up the implicit thermo-structural-mechanical welding simulation, the preprocessing software DynaWeld® [9] is used. With DynaWeld® and its features the complete model set-up for the welding simulation can be done including the definition of all necessary parameters (e.g. by using the available information of a Welding Procedure Specification (WPS)), c.f. [10]. "A specific heat source (called TSLE, c.f. Fig. 3, for further details see [11]) is used, for which the movement is only controlled by a weld path consisting of element nodes. The direction of the weld source is determined by the resultant of the element normal from both element rows forming the continuous weld path line" [2]. The subsequent forming simulation is performed with the same modeling approach using *AIRBAG_LINEAR_FLUID with LS-DYNA explicit solver for the inflation process. With this keyword a mass vs. time input can be defined to inflate a control volume, from which the resulting uniform inner forming pressure load is physically determined (c.f. [12]). Mass-scaling and time-scaling is used to optimize computation time.
All temperature-depending material values needed for the thermo-structural-mechanical welding simulation for stainless steel blanks and for aluminum fixing plates were provided within DynaWeld®, in particular for the

structural-mechanical values in terms of bilinear material curves (*MAT270). For the forming simulation the material model *MAT_PIECEWISE_LINEAR_PLASTICITY is used with a failure criterion of plastic strain limit to simulate bursting in a simple way. The values for true stress and true plastic strain were determined by an uniaxial tension test of the used stainless steel 1.4301 (AISI304).
For further details of the current modeling approach see [2].
After finishing the forming simulation, the originated tubular structure can be investigated with well-known simulation methods for the determination of its load capacity using the dynain-file for transferring all necessary information to this simulation step.

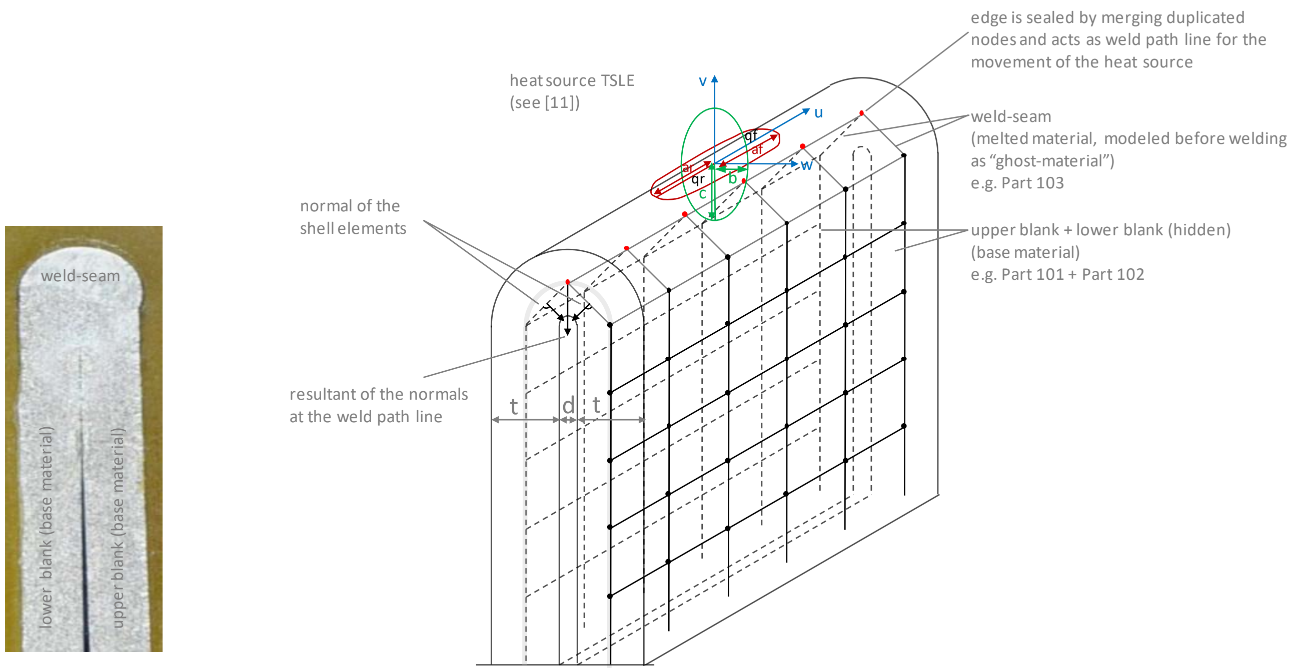

Fig. 3: Modeling scheme of a double-layered "Die-Less-Hydroforming" blank ([2], originally from [8], edited) including heat source for welding & corresponding exemplified macro-section of the edge weld, additional fixation equipment is not illustrated

3. Some results of the FEM simulation steps

When looking at the double-layered strip-shaped Die-Less-Hydroforming blank and the idea to use it as a tubular load bearing structure, some relevant simulation results are given in excerpts that relate to the characteristic phenomena described above.

3.1 Welding

For the welding of double- or multi-layered Die-Less-Hydroforming blanks two main type of welding joints are used in practice: overlap welds or edge welds. Depending on the type of weld, the corresponding weld technique is chosen. In this paper and with the corresponding modeling approach (c.f. Fig. 3) a restriction to a TIG-welding of edge welds without filler was made knowing that the chosen modeling for the weld seam can be also used for other weld techniques and weld joints. However, some adjustments of the parameters in general and of the model in detail (e.g. when a filler material is used) are needed. During welding, the two not yet jointed blanks have to be fixed with additional fixation equipment. For the following simulations plates of aluminum on both sides are used.
The welding residual stress in terms of global stress in longitudinal direction (at the middle integration point) for some strip-shaped samples with length L=965mm and width B=160mm (c.f. Fig. 5) with different configurations are given in Fig. 4. For all the configurations shown in Fig. 4, only the longitudinal seal-welds were simulated and all samples have a disturbed zone at both ends when looking to the stress plots.

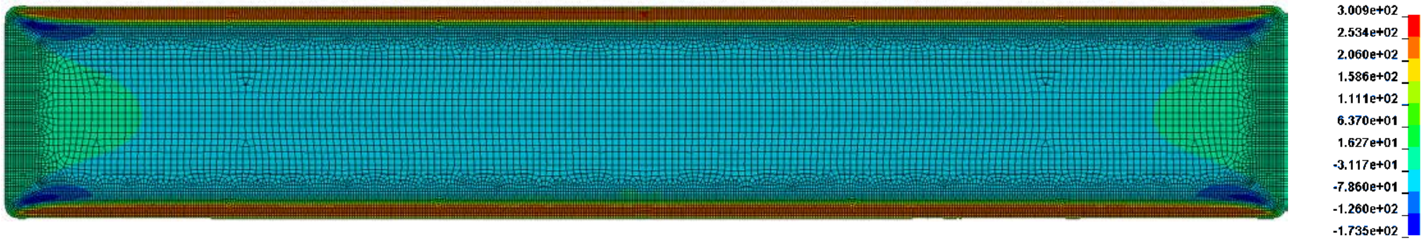

(a) Residual stress state after welding and cooling down in terms of global stress in longitudinal direction [MPa] for a sample with sheet thicknesses of 2mm with well suited regular welding

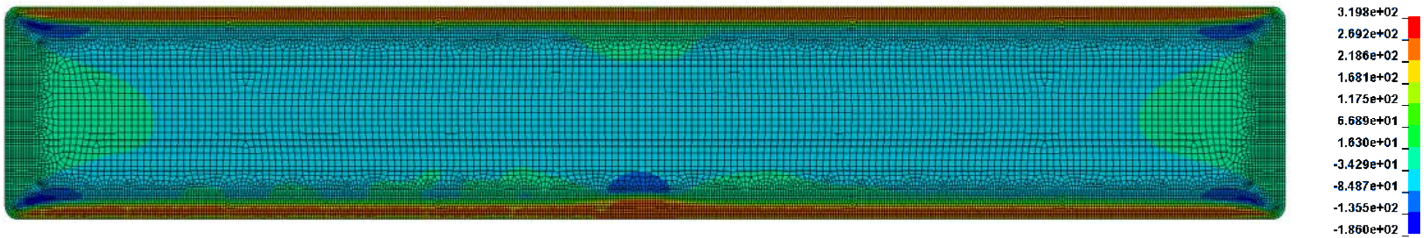

(b) Residual stress state after welding and cooling down in terms of global stress in longitudinal direction [MPa] for a sample with sheet thicknesses of 2mm with a “unmeant” heat hotspot during welding at the middle of the lower seal-weld

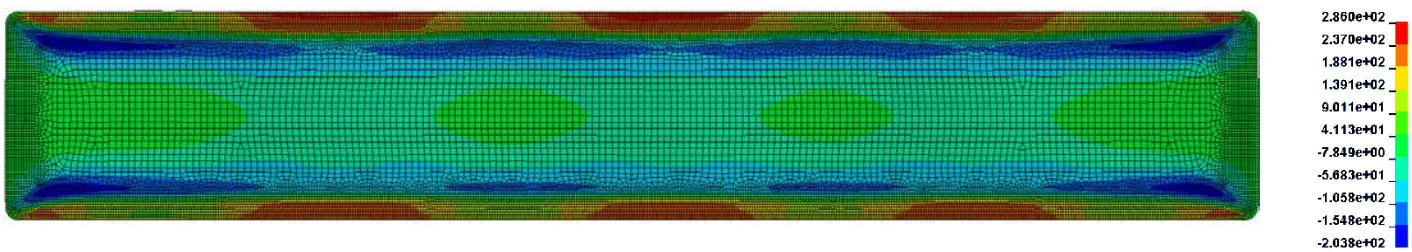

(c) Residual stress state after welding and cooling down in terms of global stress in longitudinal direction [MPa] for a sample with sheet thicknesses of 1mm showing a characteristically buckling pattern

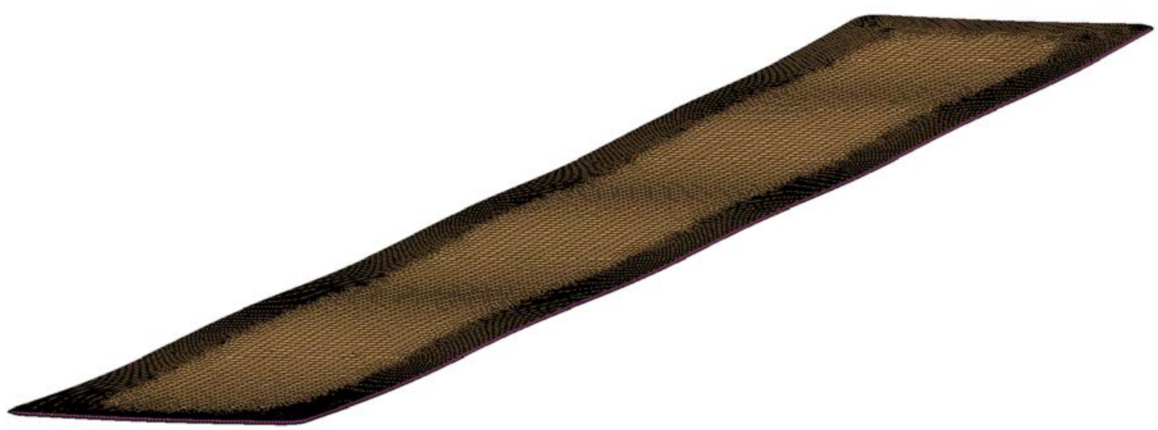

(d) 3D- view of the sample with sheet thicknesses of 1mm showing a characteristically buckling pattern

Fig. 4: Results of a thermo-structural-mechanical welding simulation after cooling down for a double-layered strip-shaped blank made of stainless steel 1.4301 (AISI304) with length L=965mm and width B=160mm

Fig. 4(a) shows an ideal welded double-layered blank, whose quality could probably only be reached in practice by an automatic welding process. The corresponding welding residual stress plot shows tension stresses near the yield strength in the weld and in the HAZ-zone. Furthermore, a large-scaled compression stress zone with apporx. 40MPa in average occurs in-between the two outer seal-welds. The welding distortion's absolute maximum is approx. 0.5mm, so that no deformation is apparently visible and this sample will be very suitable for inflation and for the later use as a tubular structure.
The sample shown in Fig. 4(b) is similar to the sample in Fig. 4(a), but has an "unmeant" heat hotspot during welding at the middle of the lower seal-weld. This is caused by a slower speed of the weld source at this position, resulting in a local increase in the energy input per unit length. Due to this, a locally concentrated increase of the compression stress occurs at this point, that could lead to a local buckle in the subsequent forming process.
When looking at the sample shown in Fig. 4(c), the thickness of both sheets is now reduced to 1mm, but the welding parameters are according to the sample of Fig. 4a with sheet thicknesses of 2mm. The welding parameters in terms of energy input per unit length of the sample in Fig. 4(a) seem to be very suitable. When reducing thickness and holding constantly the energy input per unit length, the resulting configuration shown in Fig. 4(c) will be less suited regarding the corresponding welding distortions and residual stresses because of too much energy input per unit length. This fact appears in a very inhomogeneous distribution of the welding residual stress on the one hand (c.f. Fig. 4(c)), as well as in strong welding distortions on the other hand. The welding distortions in terms of a buckling pattern are presented in Fig. 4(d) and match the welding distortions of a real strip-shaped Die-Less-Hydroforming sample presented in Fig. 1(a) very well in a qualitative way; although the dimensions and thicknesses are not identical.

3.2 Forming process

When looking at Fig. 5, an illustration of the cross section orthogonal to the longitudinal direction of the double-layered blank at different states of inflation starting from the "initial flat"-state to the "just before bursting"-state, is given. Regarding this cross section and according to [5], the distance between the two seal-welds is defined as d_{weld} and the distance between the two blanks is defined in the middle as d_{mid} at every state of inflation. With this two values and their transient development, the forming process can be described in detail. When inflating the double-layered strip-shaped blank the initially flat cross section transforms into a circle. Assuming, that the cross section transforms into a circle and no plastic membrane strain occurs in circumference direction and the highest plastic strains occur in the welding area, an ideal diameter d_{ideal} for this circlular cross section can be calculated by setting the circumference U approx. equal to two times width B. With this two values d_{weld} and d_{mid} in combination with the sheet thickness of the blank and their transient development, the forming process can be described in detail and the FEM-Simulation can be evaluated as follows.

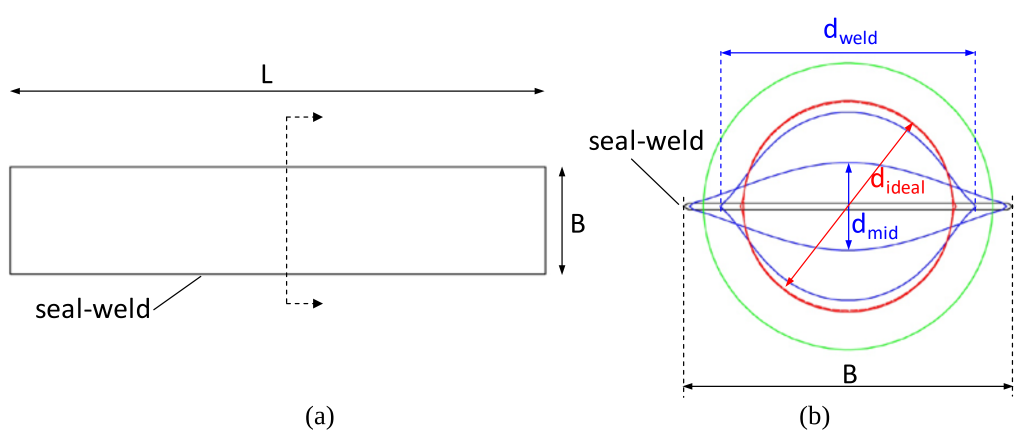

Fig. 5: Top view of the double-layered strip-shaped Die-Less-Hydroforming blank with dimensions (a) and cross section view (b) at different states of inflation as well as definition of some parameters [5]

The simulation results for the development of d_{mid} and d_{weld} versus the inner pressure load for the double-layered strip-shaped Die-Less-Hydroforming blank with a length L=965mm and a width B=160mm for different blank thicknesses ranging from 0.5mm up to 2mm and without previous welding simulation (i.e. without any distortions and residual stress at the initial state of inflation) are given in Fig. 6.
Although knowing, that the influence of the previous welding simulation for the global development of d_{mid} and d_{weld} as well as the sheet thickness will be marginal, the results for the configuration of the sample with sheet thicknesses of 2mm with well-suited regular welding (c.f. Fig. 4(a)) are implemented in Fig. 6, too.
As expected, d_{mid} starts from value 0 and d_{weld} starts from width B, whereas both values converge to the region of d_{ideal} and, after that, grow similar with increasing plastic membrane strain in circumferential direction up to final bursting. The maximum value of the bursting pressure can also be taken as the vertical path at the end of each curve from the diagram in Fig. 6 and, of course, increases with higher thickness. Additionally, the sheet thickness (of an element in the same cross section and at quarter position of width B) is also given in Fig. 6 for some chosen configurations.

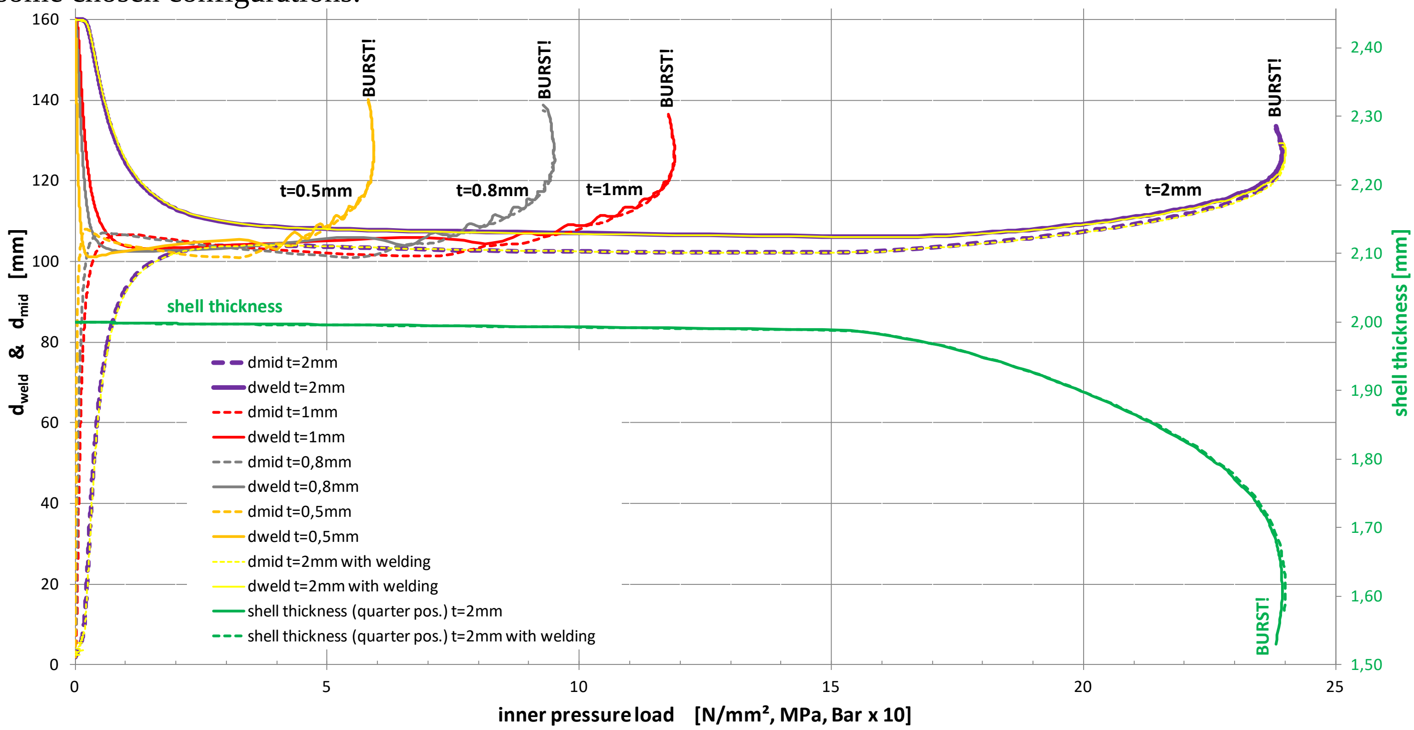

Fig. 6: Development of d_{mid}, d_{weld} and sheet thickness vs. inner forming pressure load for some configurations with or without prior welding simulation

When looking at the main benefit of the forming simulation, i.e. the possibility to determine the critical thickness for characteristically buckling phenomena (c.f. Fig. 2), the critical sheet thickness for the sample mentioned in this paper is 0.8mm determined with forming simulation without previous welding simulation.
Regarding this sample-dimension-depending buckling phenomena, the transient stress development in the longitudinal direction is given in Fig. 8 with some stress prints for discrete states of the inflation process for the sample with sheet thicknesses of 2mm as well as for the sample with the critical sheet thicknesses of 0.8mm.
During inflation, in the compression stress zone near the weld seam of the sample with sheet thicknesses of 0.8mm a critical buckling value is reached, leading to an extensive buckling pattern. A straightening effect with increasing inner forming pressure can be observed in the simulation, which leads to a complete disappearance of the buckling pattern at a later state of the inflation. The presupposition for reaching this straightening effect with a real sample is to have a working seal-weld up to this late state of the inflation process. However, this will be very difficult to reach for real samples.

Regarding the process chain simulation, the three configurations in Fig. 4 with previous welding simulations associated with the resulting welding residual stresses as well as welding distortions show characteristic behavior during the subsequent forming process.

For the configuration of Fig. 4(a) with sheet thicknesses of 2mm and previous welding simulation the transient stress development of some elements during the inflation process is given in detail in Fig. 7. It is compared to the corresponding element stress curves without previous welding simulation, whereby these curves start all at the origin. Due to the prior welding simulation and the resulting welding residual stresses, the stress curves of the chosen elements of configuration in Fig. 4(a) start already with non-zero stress values at the initial state. Those values can be seen directly on the axis of ordinate.

In general, this existing residual stress situation can lead to earlier buckling during the inflation process when at the same time the sheet thickness is near the critical value. For the sample with sheet thicknesses of 2mm with well suited regular welding (Fig. 4(a)) no buckling can be identified during the inflation simulation, because the sheet thickness is much higher than the critical value of 0.8mm. Besides that, when looking at the stress curves after reaching a circular cross section, Barlow's formula for vessels is applicable when taking into account actual diameter and sheet thickness.

Especially, when looking at the inflation process of the sample with sheet thicknesses of 2mm and an “unmeant” heat hotspot during welding at the middle of the lower seal-weld (Fig. 4(b)), a single smooth buckle can be identified in the compression zone of the hotspot during the forming simulation. Those single smooth buckles were found at some real Die-Less-Hydroforming test specimens during our research, especially when a heat input hotspot was at this position (often recognizable in terms of stronger welding discoloration at this position).

When inflating the sample with sheet thicknesses of 1mm, that has the characteristically buckling pattern from the previous welding simulation (Fig. 4(c)), there is a strong influence of these imperfections on the forming process. On the one hand, some buckles manifest in the middle field of the blank (qualitatively similar to the behavior in Fig. 1) and on the other hand, a strip-shaped buckling zone occurs near the seal-weld. The later is also qualitatively similar to the buckling pattern of Fig. 8(b), but already manifests with sheet thicknesses of 1mm, because of the strong imperfections described above.

Finally, after finishing the forming simulation, the originated model has to be prepared for the transfer to any arbitrary load capacity simulation.

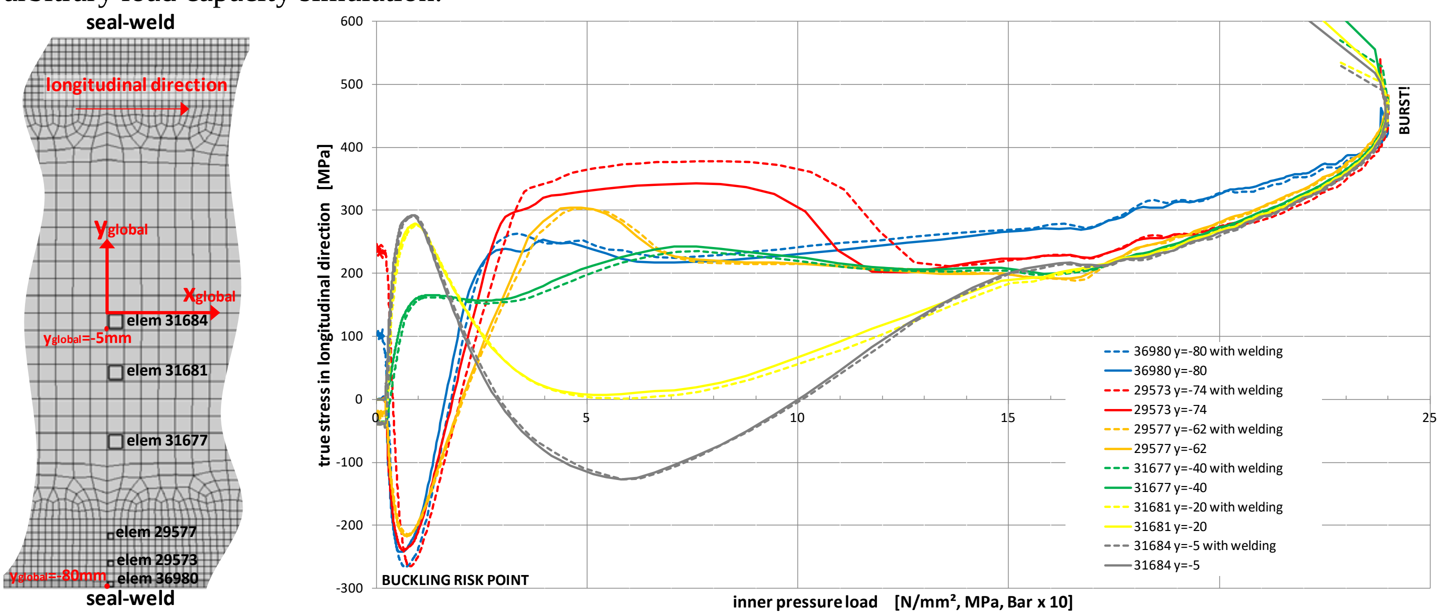

Fig. 7: Development of true stress in longitudinal sample direction vs. inner forming pressure load for configuration with or without prior welding simulation for some elements from weld seam (pos. -80) to the middle of the blank width (pos.-5) including illustration of the size-graded mesh

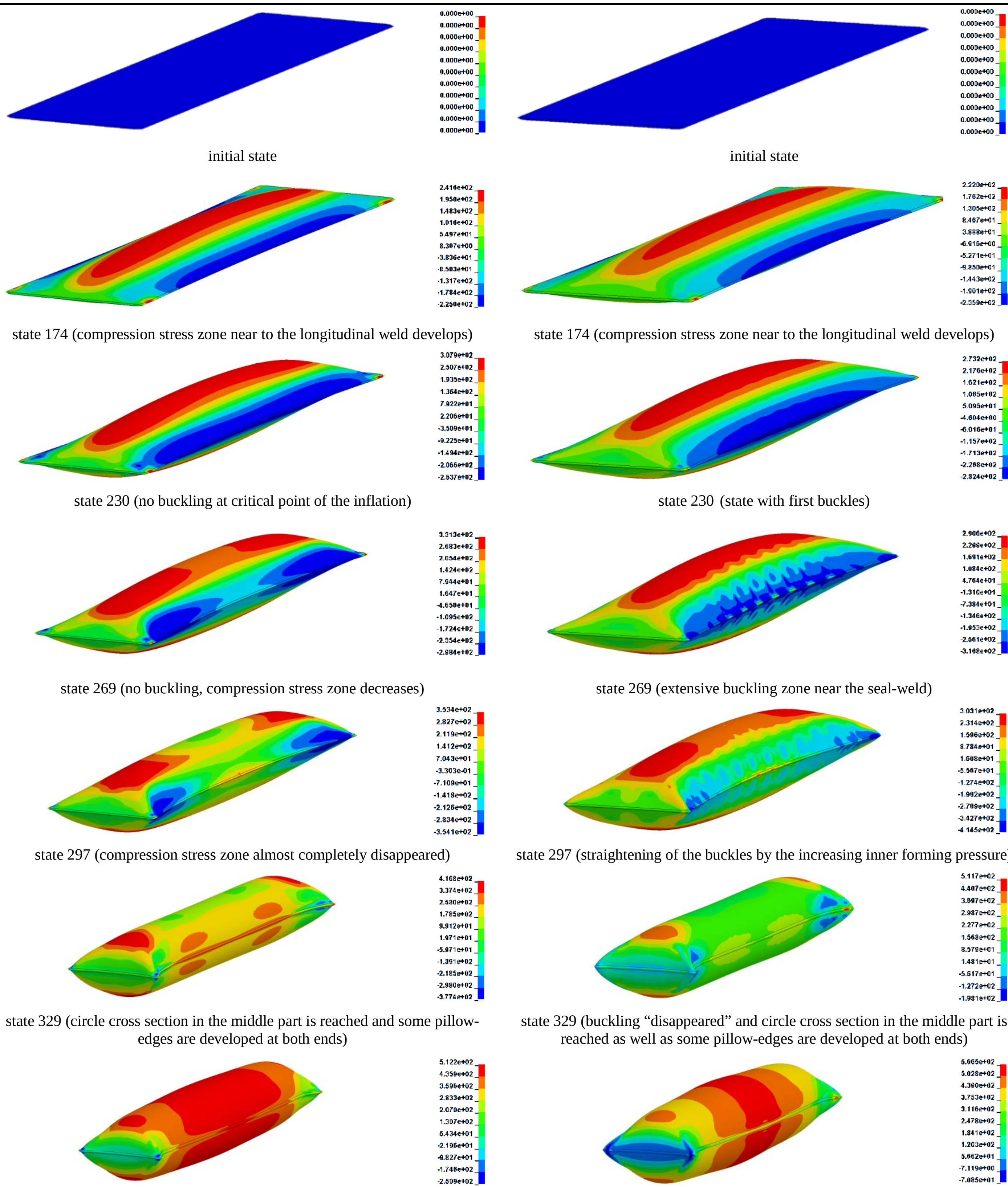

(a)	(b)
initial state	initial state
state 174 (compression stress zone near to the longitudinal weld develops)	state 174 (compression stress zone near to the longitudinal weld develops)
state 230 (no buckling at critical point of the inflation)	state 230 (state with first buckles)
state 269 (no buckling, compression stress zone decreases)	state 269 (extensive buckling zone near the seal-weld)
state 297 (compression stress zone almost completely disappeared)	state 297 (straightening of the buckles by the increasing inner forming pressure)
state 329 (circle cross section in the middle part is reached and some pillow-edges are developed at both ends)	state 329 (buckling "disappeared" and circle cross section in the middle part is reached as well as some pillow-edges are developed at both ends)
state 469 ("just before bursting")	state 479 ("just before bursting")

(a) sample with sheet thicknesses of **2mm** **(b)** sample with sheet thicknesses of **0.8mm**

Fig. 8: Element true stresses [MPa] in global longitudinal direction of the strip-shaped sample (midplane integration point) for different states during the inflation (with identical mass vs. time input rate)

3.1 Preparation for the load capacity simulations

Knowing for certain, that the determination of the load capacity of thin walled structures is in general an independent, sophisticated and extensive research area, the conditions for this paper offer only a brief glimpse. However, an overview can be given with special focus on the characteristics of Die-Less-Hydroforming structures and in particular on first approaches and necessary steps for integrating the simulation results of the previous steps welding and forming.
From the explicit forming simulation either with preceding welding simulation or without, the tubular Die-Less-Hydroforming structure is exported via dynain-file. The result appears as a bone-shaped shell body with a cylindrical part in the middle and pillow-corners at both ends. These end pieces are cut away in the following step and the custom-made tubular structure results, including all information like mesh, thickness, stresses and strains. However, this explicit forming simulation with the Airbag-Model (with mass vs. time input load model) makes it necessary to add an additional load relieving step for the chosen inflated state of the structure, because the inner forming pressure load is still active when exporting. For this implicit simulation step statically determined boundary conditions have to be set-up, which is carried out at both ends of the sample. Afterwards the two ends are cut away by using the trimming procedure of the Metal Forming eZsetup Wizard of LS-PrePost. Subsequently, an additional springback step is necessary to implement the influence of the cutting step.

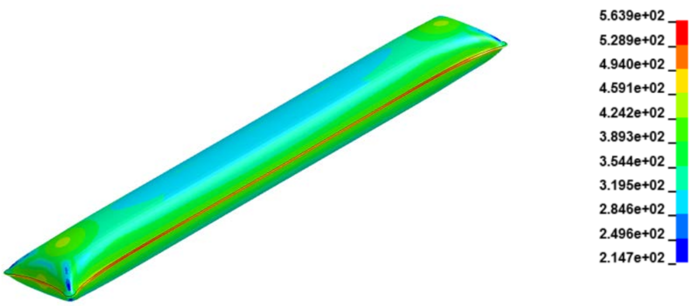

(a) bone-shaped sample pressurized inside with 142 bar

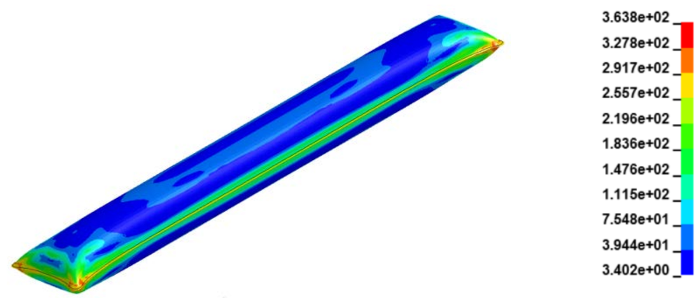

(b) unpressurized bone-shaped sample after unloading

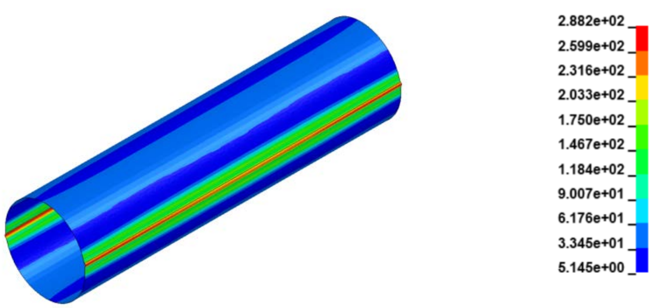

(c) tubular structure after cutting away 200mm long pieces at both ends

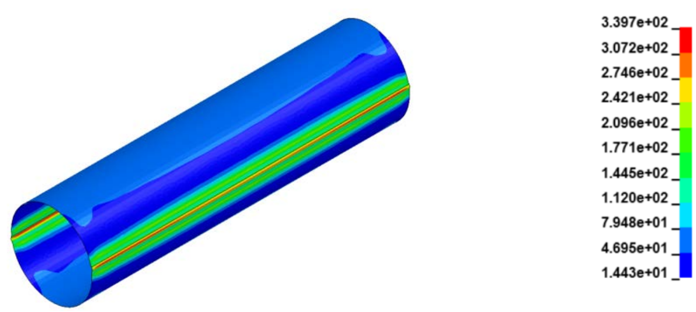

(d) spring back after the cutting step in (c)

Fig. 9: Preparation steps for a load-Capacity simulation showing v. Mises Stress [MPa] at middle integration point for the different states of preparation and the resulting tubular structure (d)

For practical application, the main task will be to choose the forming state at which the inflation has to be stopped to obtain the tubular structure. For the strip-shaped sample in this paper and the following load capacity simulation, state 329 with 142 bar (c.f. Fig. 8(a)) of inner forming pressure was identified as technically suitable. The circular cross section in the middle area of the sample is reached here, but less plastic membrane strain in circumferential direction associated with less sheet thickness reduction exists, see Fig. 6.

The resulting tubular structure inflated on basis of the double-layered blank of Fig. 4(a) with a previous welding simulation is presented in Fig. 9(a). After releasing the inner forming pressure in Fig. 9(b), after cutting away 200mm long pieces at both ends in Fig. 9(c) and after the spring-back step in Fig. 9(d), the cylindrical tubular structure results. Now it has internal equilibrium.
The resulting deformed mesh of the whole structure and in particular that of the weld seam mesh seem to match the real physical sample geometry and weld seam geometry very well compared to some real samples and their macro sections. The v. Misses stress plot shows the expected distribution according to the deformation of the forming process. Thus, the model seems to be very suitable for intensive load capacity simulation. Some first load capacity simulations with the Die-Less-Hydroforming-tubular structure (including a full or partly information transfer over the process chain) were already successfully performed, showing further research potential as described in the next chapter.

4. Summary and Outlook

A process chain simulation was presented for the two most important steps of Die-Less-Hydroforming, i.e. welding and forming, including the preparation steps for a subsequent load capacity simulation, and was successfully applied for the manufacturing of a tubular structure from an initial strip-shaped double-layered blank. According to the original idea, a tubular structure with a circular cross section is achieved, but when exporting the structure at earlier states, e.g. where the cross section is elliptic-like, it can be interesting for building applications, e.g. for sword-shaped columns. Depending on the respective use of the structure, any arbitrary load capacity simulation can be performed in the subsequent step, whereas the information from previous simulations steps can be taken into account if required.
Some first load capacity simulations with the resulting geometry from the process chain simulation were already performed. They are working fine and showing an immense further research demand, especially when looking at the stability simulation of the cold-formed thin walled Die-Less-Hydroforming structure with its specific longitudinal weld seams. Since the most important fabrication steps welding and forming are implemented in the process chain simulation, one question regarding the determination of the load capacity remains: is there a need to add further imperfections? If yes, is the addition of well-known standard imperfection approaches (imperfections in terms of eigenmodes from a linear buckling analysis) suitable and sufficient, or should imperfections be inserted that are directly generated via the fabrication process, e.g. by using some hot spot welding points in the simulation as natural imperfections?

Acknowledgement

Special thanks go to DynaWeld GmbH & Co. KG for the free of charge disposal of the software DynaWeld® including support.

References

[1] Geckeler, J.W.: "Plastisches Knicken der Wandung von Hohlzylindern und einige andere Faltungserscheinungen an Schalen und Blechen", Journal of Applied Mathematics and Mechanics, Volume 8, Issue 5, 1928, p. 341–352, doi: 10.1002/zamm.19280080502

[2] Metzger A., Ummenhofer, T.: "Process chain simulation for “Die-Less-Hydroforming” including welding and forming with “DynaWeld” and “LS-DYNA”", 11th European LS-DYNA Conference, Salzburg, 2017

[3] Rawlings, B.: "Inflated Ductile Metal Structures", Architectural Science Review, Volume 10, Issue 2, 1967, doi:10.1080/00038628.1967.9697103

[4] Kleiner, M., Kolleck, R., Weidner, T.: "Mobile Herstellung leichter, einfacher Stahlrohre durch Hydroformen", Forschungsbericht Düsseldorf: Verl. u. Vertriebsges. mbH (Forschung für die Praxis / Studiengesellschaft Stahlanwendung, P 354), 1998

[5] Metzger, A.: "PhD Thesis (in progress) concerning the topic of Die-Less-Hydroforming", Karlsruhe Institute of Technology, KIT Steel & Lightweight Structures, Research Center for Steel, Timber & Masonry

[6] Furze, C.: "FIREWORK SAFETY SUIT-Stand INSIDE a fireworks display", www.youtube.com, August 21, 2014, retrieved on January 31, 2018 from https://youtu.be/eA46WFX7jWA

[7] Furze, C.: "A Great technique you most likely have all the tools for", www.colinfurze.com/, undated, retrieved on January 31, 2018 from http://www.colinfurze.com/hydroforming.html

[8] Metzger, A., Ummenhofer, T.: "Schweißsimulation von „Die-Less-Hydroforming“-Platinen mit DynaWeld und LS-DYNA", in: Hildebrand, J., Loose, T. (Publisher), Tagungsband Simulationsforum 2016 Schweißen und Wärmebehandlung, Weimar, 2016, p. 148–156

[9] DynaWeld GmbH & Co. KG: "DynaWeld®", 2018, retrieved on January 31, 2018 from https://www.dynaweld.de/

[10] Loose, T.: "Schweißstruktursimulation mit DynaWeld ID-Konvention Eingangsparameter für die Simulation", PDF-Dokumentation DynaWeld, Ingenieurbüro für Schweißsimulation und Wärmebehandlungssimulation, Dr.-Ing. Tobias Loose, 2016

[11] Loose, T.: "DynaWeld Wärmequellen, PDF-Dokumentation DynaWeld", Ingenieurbüro für Schweißsimulation und Wärmebehandlungssimulation, Dr.-Ing. Tobias Loose, 2016

[12] Livermore Software Technology Corporation (LSTC): LS-DYNA Keyword User's Manual Volume I LS-DYNA R8.0 03/23/15 (r:6319), 2015